

Supplemental Figures and Methods

Multimodal LA-ICP-MS and nanoSIMS imaging enables copper mapping within photoreceptor megamitochondria in a zebrafish model of Menkes disease

Cheri M. Ackerman, Peter K. Weber,* Tong Xiao, Bao Thai, Tiffani J. Kuo, Emily Zhang, Jennifer Pett-Ridge* and Christopher J. Chang*

Supplemental Figures:

Figure S1. Optimization of fixation and coating conditions for metal imaging.

Figure S2. Standard curves for matrix-matched standards for copper LA-ICP-MS and nanoSIMS.

Figure S3. Zinc analysis of *Ca^{lgw71}* and WT embryos by LA-ICP-MS.

Figure S4. Standard curves for matrix-matched standards for zinc LA-ICP-MS and quantification of zinc images.

Figure S5. Selection of regions from mosaic Tg(Actin:TOM20-mCherry) retinas for nanoSIMS analysis

Figure S6. Binning and quantification of nanoSIMS scan cycles of copper puncta in the outer nuclear layer.

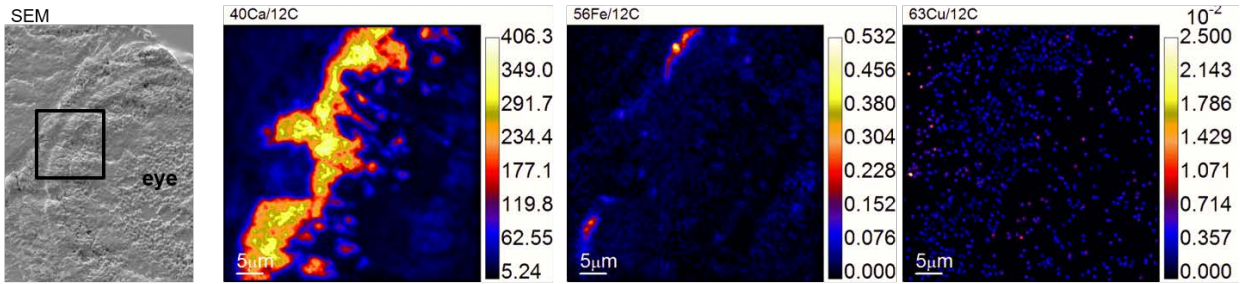
Figure S7. Electron micrographs of wildtype and *Ca^{lgw71}* embryo retinas and megamitochondria.

Figure S8. Cytochrome c oxidase activity of WT and *Ca^{lgw71}* embryos and embryo eyes.

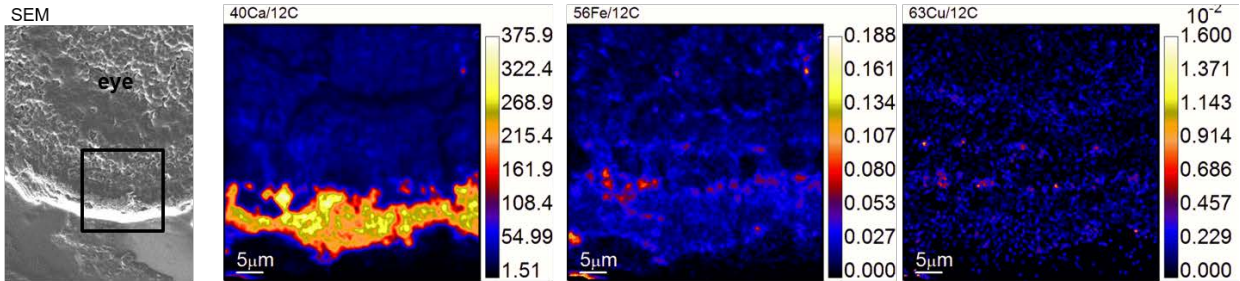
Supplemental Methods:

TOM20-iRFP gBlock

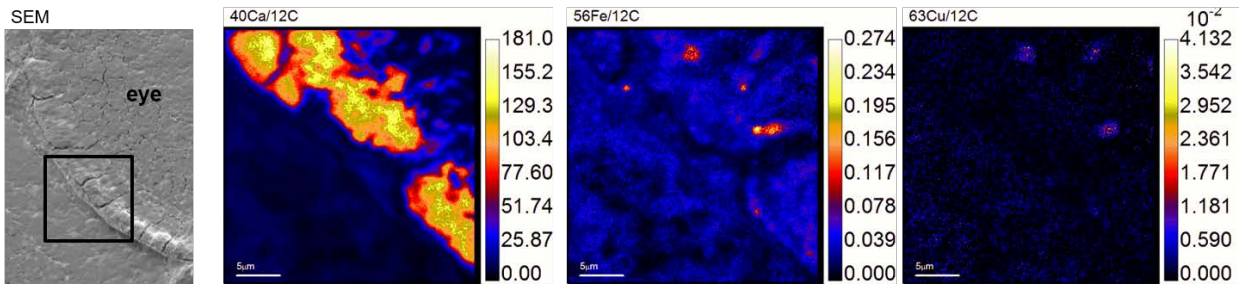
PFA-fixed; gold coating



PFA-fixed; carbon coating



Not fixed; gold coating



Not fixed; carbon coating

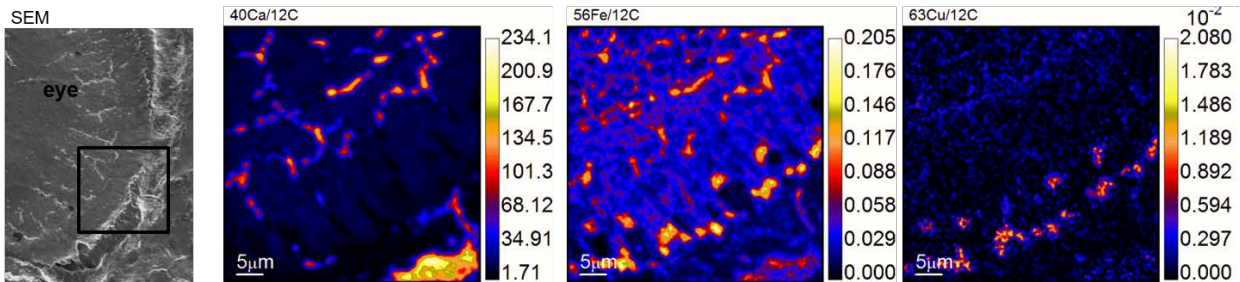


Figure S1. PFA fixation abolishes signal from copper puncta, and both carbon and gold coating yield excellent metal mapping images. Four zebrafish embryos were fixed or not fixed, as indicated, and coated with the indicated conductive substrate. SEM images (far left) confirmed retention of morphology through each coating process. Calcium signal (center left) may increase with fixation (top two rows vs bottom two rows). Both iron and copper signals (center right and far right, respectively) decrease with fixation. Copper puncta are not visible in fixed samples (far right, top two rows). Scale bars are element counts per carbon counts, scaled automatically by the LIMAGE software.

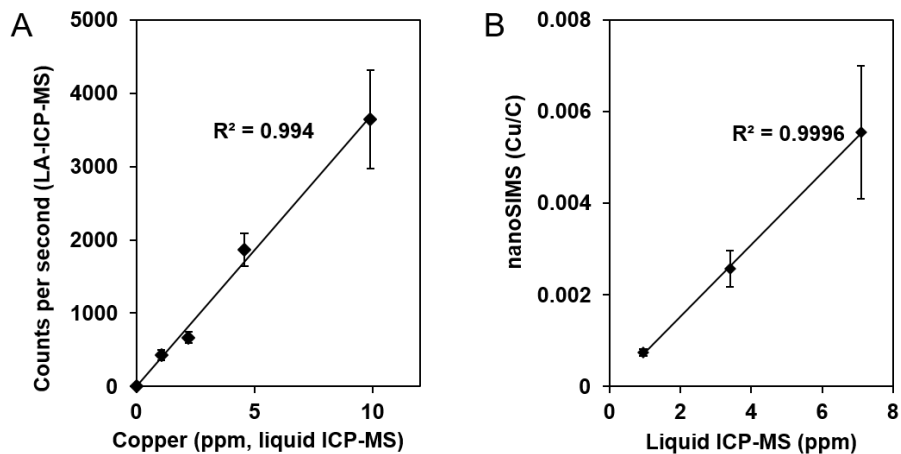


Figure S2. Standard curves for copper generated by A) LA-ICP-MS and B) nanoSIMS analysis of matrix-matched standards plotted against copper concentrations determined by liquid ICP-MS. $N \geq 3$ measurements per point. Error bars represent standard deviations.

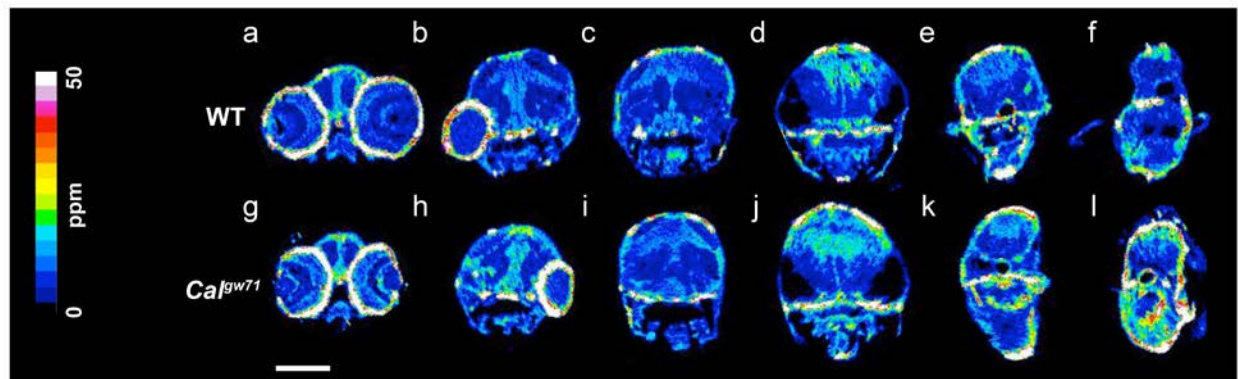


Figure S3. Zinc LA-ICP-MS images of wildtype (a-f) and *Calamity*^{gw71} (g-l) embryos (6 dpf). Scale bar: 200 μ m.

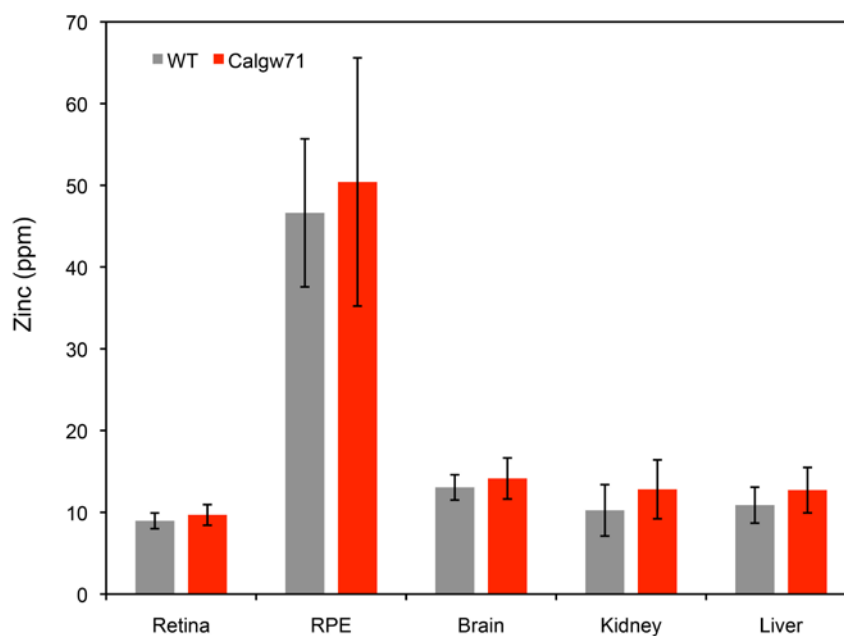


Figure S4. Quantification of zinc LA-ICP-MS images. N = 3 measurements per point. Error bars represent standard deviations. (Retina: $p=0.14$; RPE: $p=0.49$; Brain: $p=0.25$; Kidney: $p=0.25$; Liver: $p=0.32$)

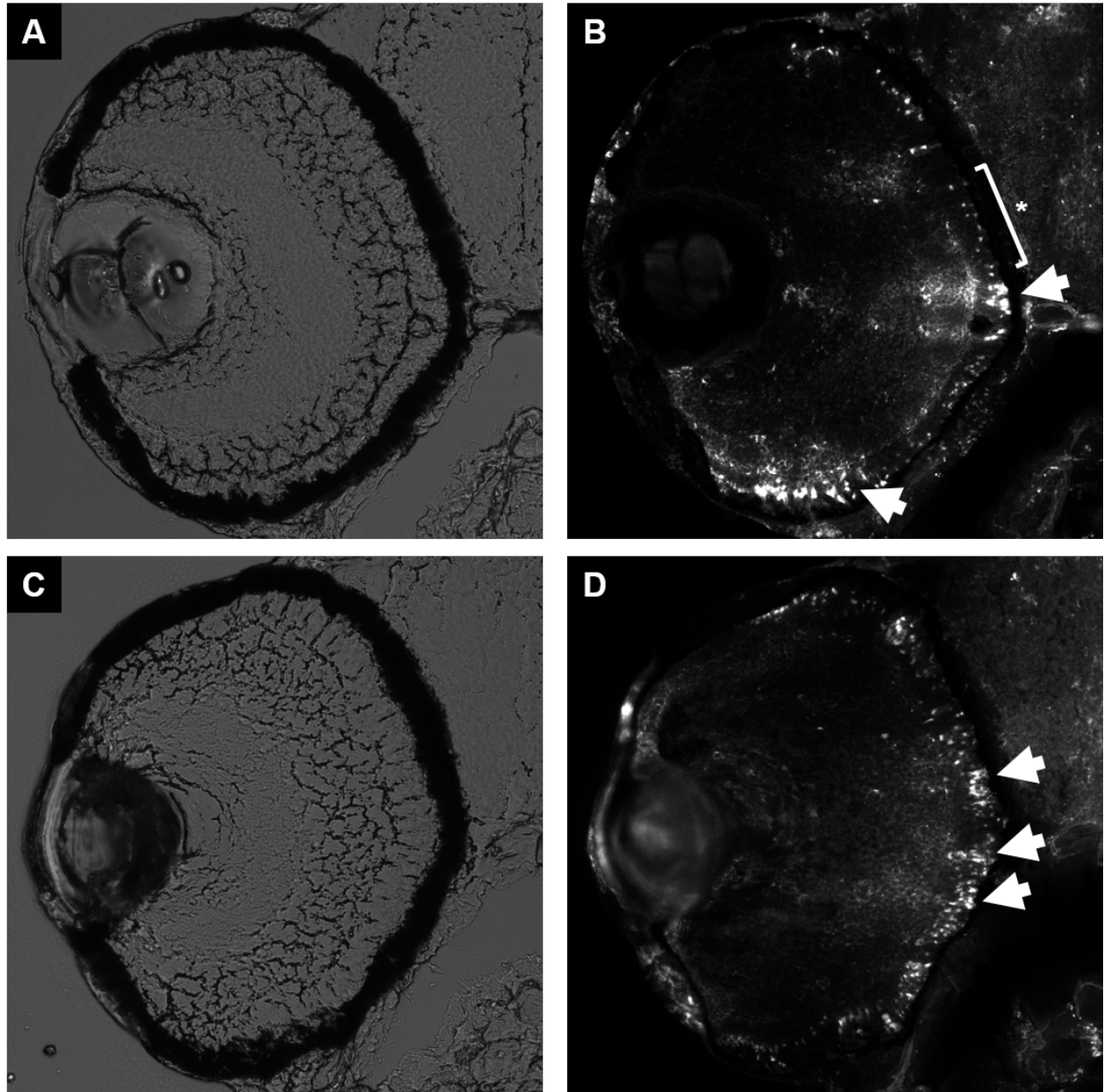


Figure S5. Selection of regions from mosaic Tg(Actin:TOM20-mCherry) zebrafish for nanoSIMS imaging. The scanned region (bracket with asterisk) was selected for the presence of labelled megamitochondria that could be clearly distinguished from one another, compared to heavily labelled regions (arrows), where fluorescence labeling of megamitochondria overlapped.

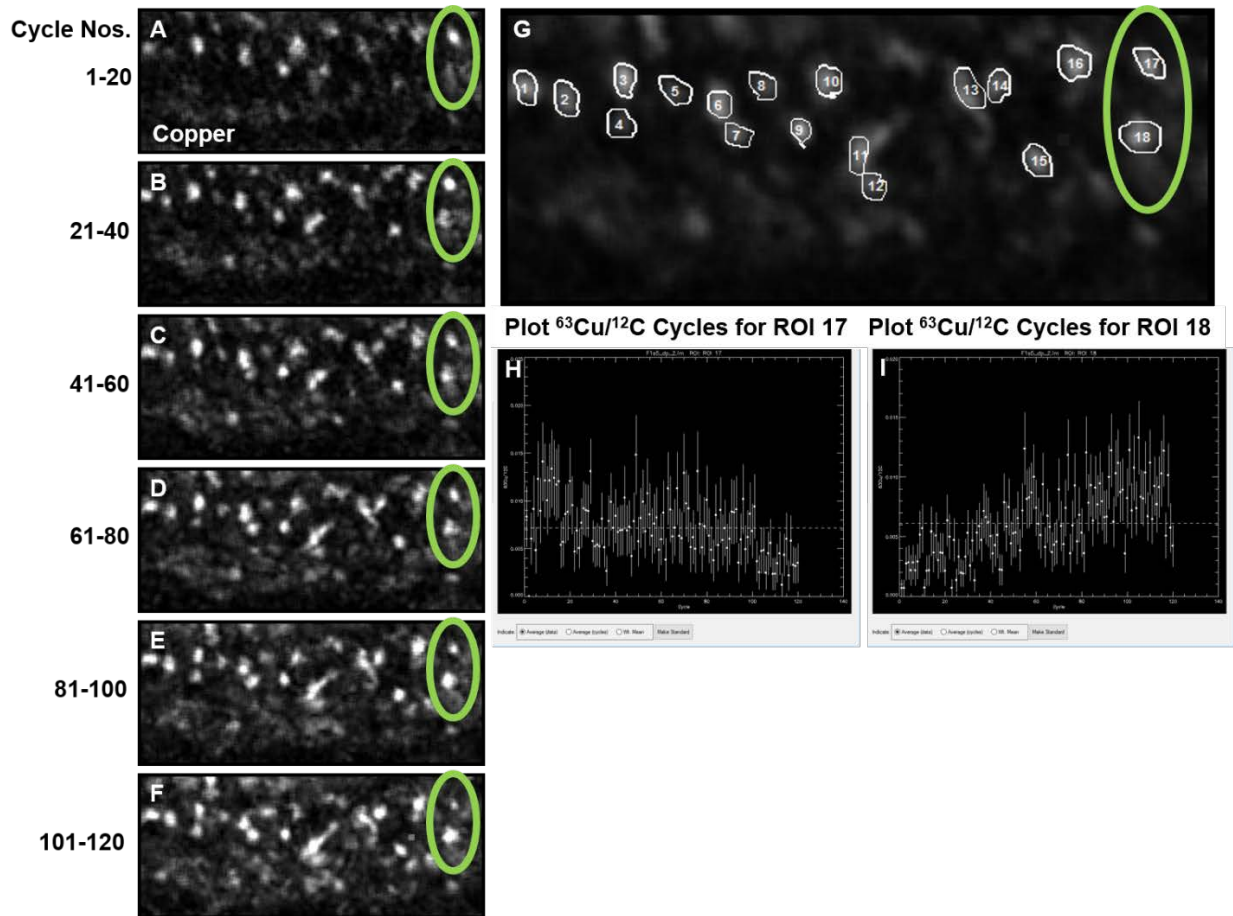


Figure S6. Binning and quantification of nanoSIMS scan cycles of copper puncta in the outer nuclear layer. nanoSIMS scan cycles were binned in groups of 20 (A-F) for illustration. Early cycles analyze the tissue surface, revealing a subset of the copper puncta contained in the tissue. Later cycles analyze deeper tissue, with a different pattern of copper puncta than earlier cycles. Regions of interest (ROIs) were drawn around copper puncta for quantification (G). ROIs #17 and #18 are circles in green. Profiles of copper counts in ROIs #17 and #18 are shown (H and I, respectively). ROI #17 shows a strong copper signal in earlier cycles, due to its location close to the surface of the tissue, while ROI #18 shows no copper signal at the tissue surface but a strong signal deeper into the tissue.

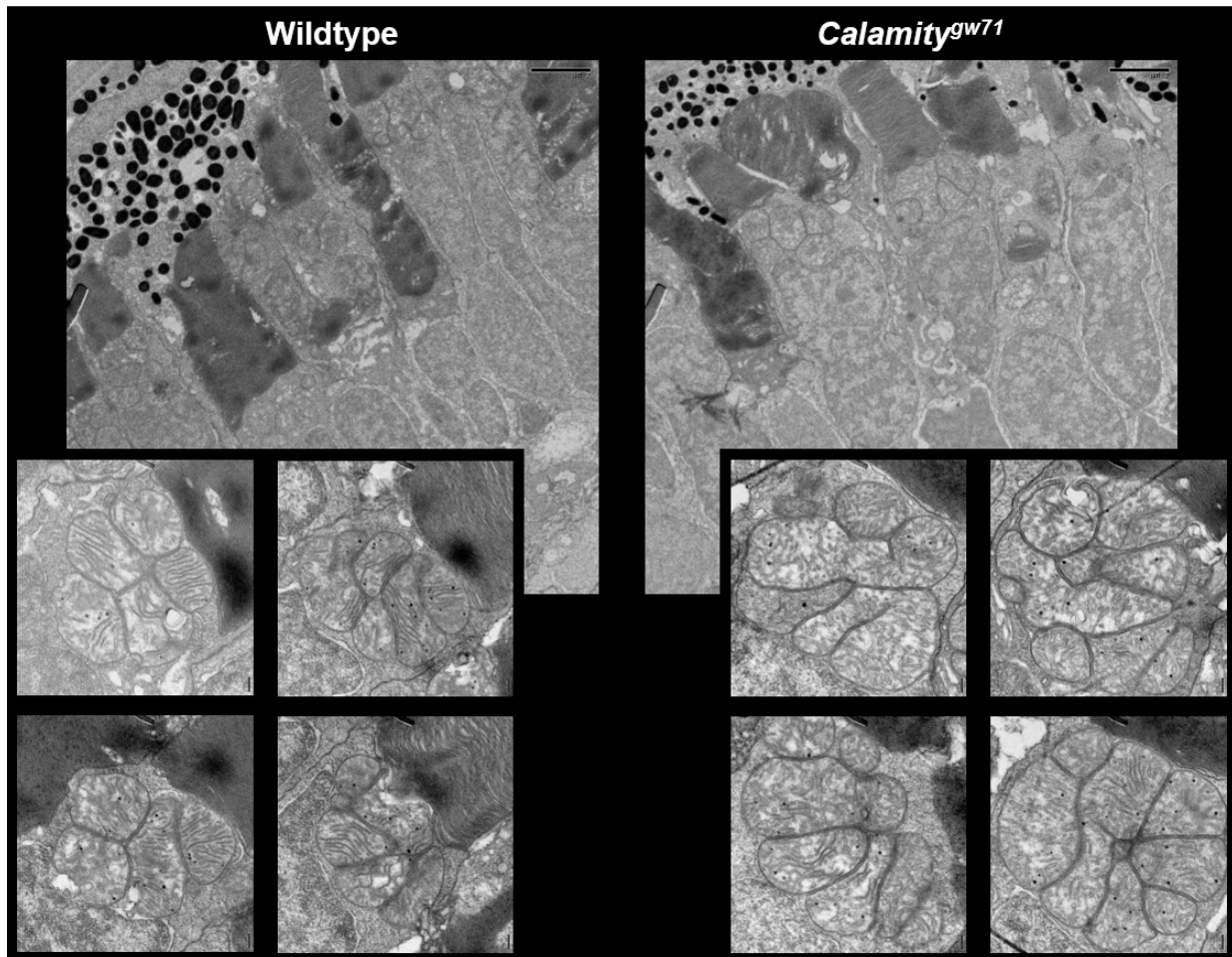


Figure S7. Electron micrographs of wildtype and *Cal^{gw71}* embryos reveal no significant morphological differences in receptor architecture (top) or megamitochondria (bottom, inset).

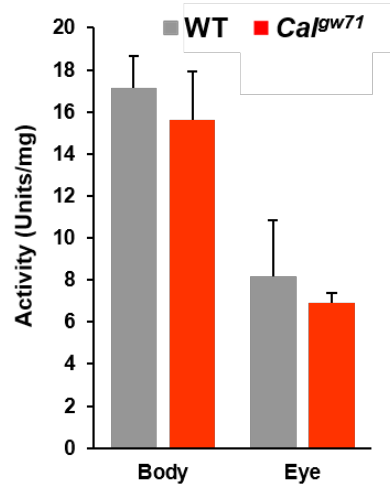


Figure S8. Cytochrome c oxidase activity in whole zebrafish embryos and zebrafish embryo eyes. Error bars represent standard deviations. Body: N = 15, $p = 0.38$; Eye: N = 3 samples, 5 eyes/sample, $p = 0.49$.

TOM20-iRFP gBlock:

The TOM20-iRFP gBlock was ordered from Integrated DNA Technologies (IDT). Overlap regions for the Gibson Assembly are highlighted in gray.

```
TGGATCATCATCGATGAATTAATTCGAGCTTTAACTCTCCAACGCCGTGATGCGCGTGGCAATT  
CTTTCTGCAAGCCGCTTACAGATGGCCCGGAGCTCAAAGCGGATAAATCGCGGCAAATAGTGAT  
GGCAAACCTACCAGTCCCCAGAGCTTGCCTCCGACGACCAATGAGACAGCCAAAGTCGCGCGGAC  
ACCCATATCCTTCAAAAACTGGAGATGACAGGGGCTCATGCTCCGAAGAAAGCAGCCTGACATA  
TCAAGGTCCCTGCCCGTCAACGGTGACAGACGTGGCTCCAGTGGAACCGGCTGGTATGTTACGT  
CTACGAGAACTCTGACTCTCTGGCGAACGTACAATTGACGTGCCATCTGAGGTACAGTGCTACT  
AGGGTATCGATTACCGAAATAGCTTTCAAGACCTGGCACGTGACACTCAGAAAAGACCAAACCG  
TGCCCCTGCTCATCGAATCTATATAACCATTACCCTGTCGTACCCCGTACACTGTTGGAACAACA  
ACACTGTGTCGTCACAGAGCGCTCGCAAAGAGCCAGCAGTTCTAATGCGTTCAAGTGCAGGTGC  
CAAAGTGCCGAAAGATCGATAGAGGGACCGGCACGTTCCAATTCTATAATCAACCCCCCTCG  
GGTGGTCGATGCATCAATCCGCAATACTCGGTGGACGGGTTACCTATTCTACACCTTACGGCGA  
CCGGCATCCCTTCAGCCGTAGGATCCAAATGGGGGAGTATCTTAATAAGAAGGTCTCCGTCTAT  
TTCAGCGAGTGGTACGCCAAGACTGAACCAAGATTGAGAACTCGGCTGCGTTGGCGCTCGCT  
TGAATTACTCTATGGTCATGCTCACTTACAACCAGCAATGCTCCGTGAGGCTGGATAGAACCTG  
CGAGATGAATTTCTTCGTGCTCGCAGTTTGAATGACTAGCGGTCCCGAAAGCGGGGCTTCCAGA  
AGCGTGGCCGGCGACAGAACCGCTGTTAGGATCTGACCGTCGTTTACGGTCAAATATATACAG  
TACCCTATGAACAGAGCCCCACAGACGCCAGCGCAATAGCAGAGTTCCGGCCCACCATGGcta  
tagtgtcacctaaataggcctagga
```